

Hadronic Parity-Violation on the Lattice

Silas R. Beane and **Martin J. Savage**

*Department of Physics, University of Washington,
Seattle, WA 98195.*

Abstract

We motivate lattice QCD studies of the parity-violating pion-nucleon coupling constant and extend flavor-conserving hadronic parity-violation from QCD to partially-quenched QCD. The parity-violating pion-nucleon coupling and the anapole form factor (and moment) of the proton are computed to one-loop order in the partially-quenched chiral expansion. For the parity-violating pion-nucleon interaction, we include the contributions from total derivative operators necessary to match the kinematics that will be used in lattice simulations.

I. INTRODUCTION

While flavor-changing parity-violating (PV) interactions are well understood theoretically and a great deal of precise data exists, knowledge of flavor-conserving parity-violation is rather primitive. Flavor-conserving parity-violation continues to be an area of intense investigation in the nuclear physics community. Its study is presently serving both to uncover the structure of the nucleon in electron-scattering experiments such as SAMPLE [1], and to determine PV flavor-conserving couplings between pions and nucleons [2,3]. The problems that are encountered in this sector are both experimental and theoretical. On the experimental side, the PV signals, unlike those in flavor-changing processes, appear as small deviations in either a strong or an electromagnetic process, such as PV in $ep \rightarrow ep$, or in the circular polarization of the γ -ray emitted in $^{18}\text{F}^* \rightarrow ^{18}\text{F}\gamma$ [3]. The current situation is somewhat confused by the fact that measurements of parity-violation in atoms and nuclei do not give rise to a consistent set of couplings between hadrons [4]. However, it is important to keep in mind that many of the “experimental” determinations of these couplings require theoretical inputs with varying degrees of reliability. Recently, it has been reemphasized that measurements of PV observables in the single-nucleon sector would significantly ameliorate the situation by eliminating many-body uncertainties [5,6]. Despite the inherent difficulty of such experiments, there are ongoing efforts to measure PV processes in systems with only one or two nucleons, such as the angular-asymmetry in $\vec{n}p \rightarrow d\gamma$ [7–9]. Such measurements should provide a reliable determination of the leading-order (LO), momentum-independent weak πNN coupling constant, $h_{\pi NN}^{(1)}$.

On the theoretical side, despite heroic efforts to model [10,11] hadronic matrix elements of the four-quark operators that appear in the low-energy effective theory of the standard model, there are no reliable calculations of the PV couplings between hadrons. A first principles calculation of $h_{\pi NN}^{(1)}$ in lattice QCD would therefore be extremely welcome. This would require a lattice QCD simulation of a correlator with three hadronic sources interacting via a four-quark operator. Unfortunately, chiral symmetry does not allow one to relate the πNN correlator to a correlator without the pion. On the bright side, the structure of the four-quark weak Hamiltonian requires a flavor change in the nucleon and therefore there are no disconnected diagrams to be computed on the lattice.

A standard difficulty in reliably computing $h_{\pi NN}^{(1)}$ on the lattice is that present computational limitations necessitate the use of lattice quark masses that are significantly larger than those of nature. In order to make a connection between lattice calculations in the foreseeable future and nature, an extrapolation in the quark masses is required. Chiral perturbation theory (χ PT) provides a systematic description of low-energy QCD near the chiral limit, and this technique has been extended to describe both quenched QCD (QQCD) [12–16] and partially-quenched QCD (PQQCD) [17,18]. The hope is that future lattice simulations can be performed with quark masses that are small enough to guarantee a convergent chiral expansion, thus allowing a meaningful extrapolation to the quark masses of nature. Recently, it has been shown how to include the low-lying octet and decuplet of baryons [19,20] into partially-quenched chiral perturbation theory (PQ χ PT) [17,18]. In this work we will present $h_{\pi NN}^{(1)}$ and the anapole moment of the proton at one-loop level in $SU(4|2)_L \otimes SU(4|2)_R$ PQ χ PT with two non-degenerate light quarks. Given that lattice simulations have on-shell particles in both the initial and final states, extraction of $h_{\pi NN}^{(1)}$ requires the injection of

energy at the weak vertex. This energy non-conservation modifies the effective field theory description of the three-point function by requiring the inclusion of operators that are total derivatives. We present a calculation of $h_{\pi NN}^{(1)}$ at the one-loop level both for the case where energy is conserved and the pion is off its mass-shell with $P_\pi^\mu = 0$, and for lattice kinematics where energy is injected at the weak vertex.

II. HADRONIC PARITY VIOLATING INTERACTIONS

The four-quark operators that contribute to flavor-conserving, low-energy PV processes can be classified by how they act in isospin space, $\Delta I = 0, 1, 2$. Their QCD evolution from the weak-scale down to the strong interaction scale has been computed previously [10,21,22]. In this work we focus on the $\Delta I = 1$ interaction, as it is only in this channel that the LO operator in the chiral expansion is momentum independent. In QCD, the effective Lagrange density for $\Delta I = 1$ interactions at the quark-level is [22,23], including strange-quark operators

$$\mathcal{L}^{\Delta I=1} = -\frac{G_F}{\sqrt{2}} \frac{\sin^2 \theta_w}{3} \sum_i \left[C_i^{(1)}(\mu) \theta_i(\mu) + S_i^{(1)}(\mu) \theta_i^{(s)}(\mu) \right] \quad , \quad (1)$$

where θ_w is the weak mixing angle, and where the four-quark operators are

$$\begin{aligned} \theta_1 &= \bar{q}^\alpha \gamma^\mu q_\alpha \bar{q}^\beta \gamma_\mu \gamma_5 \tau^3 q_\beta & , & & \theta_2 &= \bar{q}^\alpha \gamma^\mu q_\beta \bar{q}^\beta \gamma_\mu \gamma_5 \tau^3 q_\alpha \\ \theta_3 &= \bar{q}^\alpha \gamma^\mu \gamma_5 q_\alpha \bar{q}^\beta \gamma_\mu \tau^3 q_\beta & , & & \theta_4 &= \bar{q}^\alpha \gamma^\mu \gamma_5 q_\beta \bar{q}^\beta \gamma_\mu \tau^3 q_\alpha \\ \theta_1^{(s)} &= \bar{s}^\alpha \gamma^\mu s_\alpha \bar{q}^\beta \gamma_\mu \gamma_5 \tau^3 q_\beta & , & & \theta_2^{(s)} &= \bar{s}^\alpha \gamma^\mu s_\beta \bar{q}^\beta \gamma_\mu \gamma_5 \tau^3 q_\alpha \\ \theta_3^{(s)} &= \bar{s}^\alpha \gamma^\mu \gamma_5 s_\alpha \bar{q}^\beta \gamma_\mu \tau^3 q_\beta & , & & \theta_4^{(s)} &= \bar{s}^\alpha \gamma^\mu \gamma_5 s_\beta \bar{q}^\beta \gamma_\mu \tau^3 q_\alpha \quad , \end{aligned} \quad (2)$$

and their coefficients at the chiral symmetry breaking scale are [22,23]

$$\begin{aligned} C^{(1)}(\Lambda_\chi) &= (1.10 , 0.068 , 0.234 , -0.697) \\ S^{(1)}(\Lambda_\chi) &= (5.61 , -1.90 , 4.74 , -2.67) \quad , \end{aligned} \quad (3)$$

where we have neglected inter-generational mixing through the Cabibbo angle. In the limit of vanishing θ_w and degenerate quark weak-isospin doublets, the standard model possesses a global symmetry that forbids $\Delta I = 1, 2$ parity-violation [22]. This symmetry is reflected in the relative magnitudes of the $S^{(1)}$ versus the $C^{(1)}$. If strange quarks were to play no role in the structure of the nucleon, two-flavor lattice QCD simulations would provide an accurate calculation of the matrix elements of $\theta_{1,4}$, but to the extent to which strange matrix elements are non-zero, the two-flavor simulations provide only part of the PV matrix elements. The role that strange quarks may play in these matrix elements has been considered in various unjustified approaches, e.g. Ref. [10], [22] and [24], and the strange quark is found to make a sizable contribution [24] to the PV momentum independent interaction, $h_{\pi NN}^{(1)}$. However, the computation of these matrix elements in two-flavor simulations will be a vital first-step towards a rigorous understanding of flavor conserving, hadronic parity-violation.

In order to match onto a chiral Lagrange density that describes low-energy PV processes, it is convenient to introduce the objects $X_{L,R}^a$, defined as [23]

$$X_L^a = \xi^\dagger \tau^a \xi \quad , \quad X_R^a = \xi \tau^a \xi^\dagger \quad , \quad (4)$$

where

$$\xi = \exp\left(\frac{i M}{f}\right) \quad , \quad M = \begin{pmatrix} \pi^0/\sqrt{2} & \pi^+ \\ \pi^- & -\pi^0/\sqrt{2} \end{pmatrix} \quad , \quad (5)$$

and where $\xi \rightarrow L\xi U^\dagger = U\xi R^\dagger$, and $X_{L,R}^a \rightarrow UX_{L,R}^a U^\dagger$ under chiral transformations. In our convention, the pion decay constant, $f = 132$ MeV. At LO in the chiral expansion, $\Delta I = 1$ PV couplings between the pions, the nucleons and the Δ 's are described by the Lagrange density [23]¹,

$$\begin{aligned} \mathcal{L}_{\text{wk}} &= -h_{\pi NN}^{(1)} \frac{f}{4} \bar{N} [X_L^3 - X_R^3] N - h_{\pi\Delta\Delta}^{(1)} \frac{f}{4} \bar{T}^{abc,\mu} [X_L^3 - X_R^3]_c^d T_{abd,\mu} \\ &\rightarrow i\pi^- \left[h_{\pi NN}^{(1)} \bar{n}p + \frac{h_{\pi\Delta\Delta}^{(1)}}{\sqrt{3}} \bar{\Delta}^{+\mu} \Delta_{\mu}^{++} + \frac{2h_{\pi\Delta\Delta}^{(1)}}{3} \bar{\Delta}^{0\mu} \Delta_{\mu}^+ + \frac{h_{\pi\Delta\Delta}^{(1)}}{\sqrt{3}} \bar{\Delta}^{-\mu} \Delta_{\mu}^0 \right] + \text{h.c.} . \end{aligned} \quad (6)$$

III. EXTENSION TO PARTIALLY-QUENCHED QCD

The extension of the PV flavor-conserving weak operators from QCD to PQQCD is analogous to the extension of strangeness-changing operators, as discussed in detail in Ref. [26]. It is convenient to rewrite the operators in eq. (2) in terms of operators with well-defined properties under chiral transformations. Neglecting the strange-quark operators one finds,

$$\begin{aligned} \tilde{\theta}_1 &= \bar{q}^\alpha \tau^3 \gamma^\mu (1 - \gamma_5) q_\alpha \bar{q}^\beta \gamma_\mu (1 - \gamma_5) q_\beta \quad , \quad \tilde{\theta}_2 = \bar{q}^\alpha \tau^3 \gamma^\mu (1 + \gamma_5) q_\alpha \bar{q}^\beta \gamma_\mu (1 - \gamma_5) q_\beta \\ \tilde{\theta}_3 &= \bar{q}^\alpha \tau^3 \gamma^\mu (1 - \gamma_5) q_\alpha \bar{q}^\beta \gamma_\mu (1 + \gamma_5) q_\beta \quad , \quad \tilde{\theta}_4 = \bar{q}^\alpha \tau^3 \gamma^\mu (1 + \gamma_5) q_\alpha \bar{q}^\beta \gamma_\mu (1 + \gamma_5) q_\beta \quad , \end{aligned} \quad (7)$$

and operators $\tilde{\theta}_5 \dots \tilde{\theta}_8$, corresponding to the other color-contraction. These objects transform as $(\mathbf{3}, \mathbf{1})$, $(\mathbf{1}, \mathbf{3})$, $(\mathbf{3}, \mathbf{1})$, $(\mathbf{1}, \mathbf{3})$, respectively under $SU(2)_L \otimes SU(2)_R$ chiral transformations. The most general extension of this operator set to PQQCD is quite messy, as one ends up dealing with objects of the form (\mathbf{A}, \mathbf{A}) of $SU(4|2)_L \otimes SU(4|2)_R$, where \mathbf{A} denotes the adjoint representation of $SU(4|2)$. Therefore, for simplicity reasons alone, we will only consider extensions of the form $(\mathbf{A}, \mathbf{1})$ and $(\mathbf{1}, \mathbf{A})$ ². In this case, we can define the weak flavor matrix

$$\vec{\tau}^3 = (1, -1, h_j, h_l, h_j, h_l) \quad , \quad (8)$$

where h_j and h_l are arbitrary weak charges. This matrix is supertraceless and its matrix elements reduce to those of QCD when the sea-quark (j and l) masses become degenerate

¹Ref. [25] uses similar notation with $h_{\pi NN}^{(1)} = h_\pi$ and $h_{\pi\Delta\Delta}^{(1)} = h_\Delta$.

²The flavor structure can be further extended when lattice simulations require.

with the valence-quark masses. The quark mass matrix in PQCD is given by $m_Q = \text{diag}(m_u, m_d, m_j, m_l, m_u, m_d)$. Further, in analogy with QCD [23] we define

$${}^{(PQ)}X_L^a = \xi^\dagger \bar{\tau}^a \xi \quad , \quad {}^{(PQ)}X_R^a = \xi \bar{\tau}^a \xi^\dagger \quad . \quad (9)$$

The LO Lagrange density describing the low-energy PV interactions in PQ χ PT is

$$\begin{aligned} \mathcal{L}_{\text{wk}} = & -W_1 \frac{f}{4} \left(\bar{\mathcal{B}} \mathcal{B} \left[{}^{(PQ)}X_L^3 - {}^{(PQ)}X_R^3 \right] \right) - W_2 \frac{f}{4} \left(\bar{\mathcal{B}} \left[{}^{(PQ)}X_L^3 - {}^{(PQ)}X_R^3 \right] \mathcal{B} \right) \\ & - W_3 \frac{f}{4} \left(\bar{\mathcal{T}}^\nu \left[{}^{(PQ)}X_L^3 - {}^{(PQ)}X_R^3 \right] \mathcal{T}_\nu \right) , \end{aligned} \quad (10)$$

where \mathcal{B} , which contains the nucleons, and \mathcal{T}_ν , which contains the Δ -resonances, transform in the **70** and **44** representations of $SU(4|2)$, respectively [20]. The contraction of flavor indices, $(\)$, can be found in Ref. [15]. At tree-level one can make the identification

$$h_{\pi NN}^{(1)} = \frac{1}{3} (2W_1 - W_2) \quad , \quad h_{\pi\Delta\Delta}^{(1)} = W_3 \quad . \quad (11)$$

The LO weak coupling between the nucleons and Δ -resonances involves one derivative and hence is higher order in the chiral expansion.

The Lagrange density describing the parity-conserving interactions of the **70** and **44** with the pseudo-Goldstone bosons at LO in the chiral expansion is [15],

$$\begin{aligned} \mathcal{L} = & 2\alpha \left(\bar{\mathcal{B}} S^\mu \mathcal{B} A_\mu \right) + 2\beta \left(\bar{\mathcal{B}} S^\mu A_\mu \mathcal{B} \right) + 2\mathcal{H} \left(\bar{\mathcal{T}}^\nu S^\mu A_\mu \mathcal{T}_\nu \right) \\ & + \sqrt{\frac{3}{2}} \mathcal{C} \left[\left(\bar{\mathcal{T}}^\nu A_\nu \mathcal{B} \right) + \left(\bar{\mathcal{B}} A^\nu \mathcal{T}_\nu \right) \right] , \end{aligned} \quad (12)$$

where S^μ is the covariant spin-vector [27–29], and $A^\mu = \frac{i}{2} \left(\xi \partial^\mu \xi^\dagger - \xi^\dagger \partial^\mu \xi \right)$. A comparison with the LO interaction Lagrange density of QCD yields the tree-level identification [20]

$$\alpha = \frac{4}{3} g_A + \frac{1}{3} g_1 \quad , \quad \beta = \frac{2}{3} g_1 - \frac{1}{3} g_A \quad , \quad \mathcal{H} = g_{\Delta\Delta} \quad , \quad \mathcal{C} = -g_{\Delta N} \quad , \quad (13)$$

where g_A , $g_{\Delta\Delta}$ and $g_{\Delta N}$ are the NN , $\Delta\Delta$ and ΔN isovector axial couplings, respectively, and $(g_A + g_1)$ is the isosinglet axial coupling. For details about this and other aspects of PQ χ PT, we refer the reader to Ref. [20].

IV. $h_{\pi NN}^{(1)}$ AT ONE LOOP WITH $P_\pi^\mu = 0$

In QCD, the LO pion-nucleon PV interaction is generated by the Lagrange density in eq. (6). At higher orders, the PV pion-nucleon interaction will receive contributions from one-loop diagrams and also from terms at next-to-LO (NLO) in the chiral expansion involving a single insertion of m_q ,

$$\mathcal{L} = -\tilde{c}_1 \frac{f}{4} \bar{N} \{ \mathcal{M}_+^{QCD}, X_L^3 - X_R^3 \} N - \tilde{c}_2 \frac{f}{4} \bar{N} \left(X_L^3 - X_R^3 \right) N \text{tr} \left(\mathcal{M}_+^{QCD} \right) \quad . \quad (14)$$

Since the pion mass is much greater than the proton-neutron mass difference, one does not have all three particles on their mass-shells. Therefore, we compute the one-loop corrections to the weak vertex in both QCD and PQQCD. The one-loop calculation of the vertex has been performed previously in QCD [25], and explicit computation in the isospin limit and with vanishing pion four-momentum, P_π^μ , gives

$$\begin{aligned} \Gamma_{\bar{n}p\pi^+} = & -h_{\pi NN}^{(1)} - 2\bar{m} (\tilde{c}_1 + \tilde{c}_2) \\ & + \frac{1}{16\pi^2 f^2} \left[h_{\pi NN}^{(1)} \left(\frac{2}{3} + \frac{3}{2} g_A^2 \right) L_\pi + h_{\pi\Delta\Delta}^{(1)} \frac{20}{9} g_{\Delta N}^2 J_\pi \right] , \end{aligned} \quad (15)$$

where $\bar{m} = m_u = m_d$ in the isospin limit. The loop functions are defined as $L_\pi = m_\pi^2 \log(m_\pi^2/\mu^2)$, and $J_\pi = J(m_\pi, \Delta, \mu)$ with

$$J(m, \Delta, \mu) = \left(m^2 - 2\Delta^2 \right) \log \left(\frac{m^2}{\mu^2} \right) + 2\Delta \sqrt{\Delta^2 - m^2} \log \left(\frac{\Delta - \sqrt{\Delta^2 - m^2 + i\epsilon}}{\Delta + \sqrt{\Delta^2 - m^2 + i\epsilon}} \right) , \quad (16)$$

and Δ is the Δ -nucleon mass splitting. Our results agree with those of Ref. [25], once differences in conventions are accounted for.

In PQQCD the counterterms involving a single insertion of m_Q that contribute to the PV pion-nucleon interaction at the one-loop level are

$$\begin{aligned} \mathcal{L}^{(ct)} = & -\frac{f}{2} \left[c_1 \bar{\mathcal{B}}^{kji} \{ (PQ) X_L^3 - (PQ) X_R^3, \mathcal{M}_+ \}_i^n \mathcal{B}_{njk} \right. \\ & + c_2 (-)^{(\eta_i + \eta_j)(\eta_k + \eta_n)} \bar{\mathcal{B}}^{kji} \{ (PQ) X_L^3 - (PQ) X_R^3, \mathcal{M}_+ \}_k^n \mathcal{B}_{ijn} \\ & + c_3 (-)^{\eta_i(\eta_j + \eta_n)} \bar{\mathcal{B}}^{kji} \left((PQ) X_L^3 - (PQ) X_R^3 \right)_i^l (\mathcal{M}_+)_j^n \mathcal{B}_{lnk} \\ & + c_4 (-)^{\eta_i \eta_j} \bar{\mathcal{B}}^{kji} \left(\left((PQ) X_L^3 - (PQ) X_R^3 \right)_i^l (\mathcal{M}_+)_j^n + (\mathcal{M}_+)_i^l \left((PQ) X_L^3 - (PQ) X_R^3 \right)_j^n \right) \mathcal{B}_{nlk} \\ & + c_5 (-)^{\eta_i(\eta_l + \eta_j)} \bar{\mathcal{B}}^{kji} \left((PQ) X_L^3 - (PQ) X_R^3 \right)_j^l (\mathcal{M}_+)_i^n \mathcal{B}_{nlk} \\ & + c_6 \bar{\mathcal{B}}^{kji} \left((PQ) X_L^3 - (PQ) X_R^3 \right)_i^l \mathcal{B}_{ljk} \text{str}(\mathcal{M}_+) \\ & + c_7 (-)^{(\eta_i + \eta_j)(\eta_k + \eta_n)} \bar{\mathcal{B}}^{kji} \left((PQ) X_L^3 - (PQ) X_R^3 \right)_k^n \mathcal{B}_{ijn} \text{str}(\mathcal{M}_+) \\ & \left. + c_8 \bar{\mathcal{B}}^{kji} \mathcal{B}_{ijk} \text{str} \left(\left((PQ) X_L^3 - (PQ) X_R^3 \right) \mathcal{M}_+ \right) \right] , \end{aligned} \quad (17)$$

where $\mathcal{M}_+ = \frac{1}{2} (\xi^\dagger m_Q \xi^\dagger + \xi m_Q \xi)$. The vertex at one-loop level can be written as

$${}^{(PQ)}\Gamma_{\bar{n}p\pi^+} = \rho + \frac{1}{16\pi^2 f^2} \left(\eta^0 + h_j \eta^j + h_l \eta^l \right) + c^0 + h_j c^j + h_l c^l , \quad (18)$$

where the diagrams in Fig. 1 give

$$\begin{aligned} \rho = & -\frac{1}{3} (2W_1 - W_2) \\ \eta^0 = & -\frac{\rho}{6} [L_{ju} + L_{jd} + L_{lu} + L_{ld} + R_{\eta_u, \eta_u} + R_{\eta_d, \eta_d} - 2R_{\eta_u, \eta_d}] + \rho \, 3g_A^2 R_{\eta_u, \eta_d} \\ & + \frac{g_1 g_A}{4} [(W_1 - 2W_2) (2L_{ud} - L_{jd} - L_{ju} - L_{ld} - L_{lu}) \end{aligned}$$

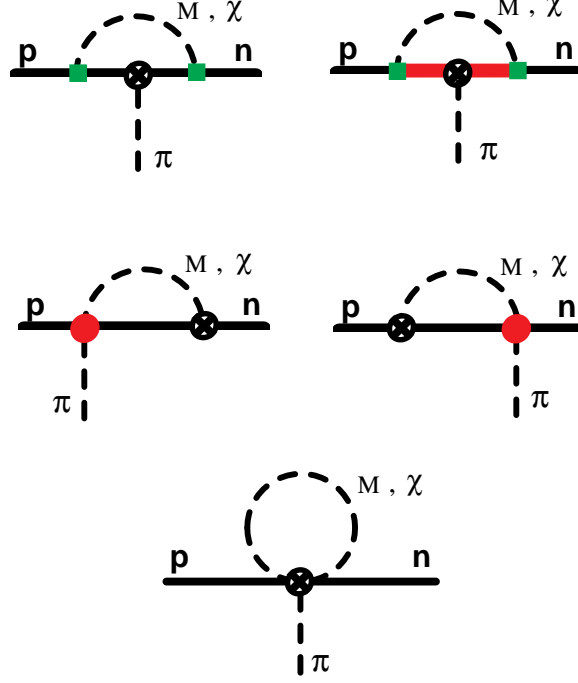


FIG. 1. One-loop graphs that give contributions of the form $\sim m_Q \log m_Q$ to the momentum independent parity-violating interaction $h_{\pi NN}^{(1)}$. A solid, thick-solid and dashed line denote a **70**-nucleon, **44**-resonance, and a meson, respectively. The solid-squares denote an axial coupling given in eq.(12), while the crossed circle denotes an insertion of the parity-violating pion-nucleon operators with coefficients $W_{1,2,3}$ in eq. (10). The solid circle denotes an insertion of the strong two-pion vertex from the nucleon kinetic energy term.

$$\begin{aligned}
& +6\rho (R_{\eta_u, \eta_u} + 2R_{\eta_u, \eta_d} + R_{\eta_d, \eta_d}) - 3W_1 (L_{uu} + L_{dd}) \\
& - \frac{g_1^2}{8} [(W_1 - 2W_2) (L_{uu} + L_{dd}) - 6\rho (R_{\eta_u, \eta_u} + 2R_{\eta_u, \eta_d} + R_{\eta_d, \eta_d}) \\
& \quad + 3W_1 (L_{ju} + L_{jd} + L_{lu} + L_{ld} - 2L_{ud})] \\
& + g_{\Delta N}^2 \frac{2}{9} W_3 (J_{dd} + J_{uu} + 4J_{ud} + J_{jd} + J_{ju} + J_{ld} + J_{lu} \\
& \quad + 2\mathcal{T}_{\eta_u, \eta_u} + 2\mathcal{T}_{\eta_d, \eta_d} - 4\mathcal{T}_{\eta_u, \eta_d}) \\
\eta^j & = \eta^l = 0 \\
c^0 & = -(m_u + m_d) \frac{1}{3} (-2c_1 + 4c_2 - c_3 - c_4 + 2c_5) - (m_j + m_l) \frac{2}{3} (-c_6 + 2c_7) \\
c^j & = c^l = 0 \quad , \tag{19}
\end{aligned}$$

where $R_{x,y} = \mathcal{H}(L_x, L_y, L_X)$ and $\mathcal{T}_{x,y} = \mathcal{H}(J_x, J_y, J_X)$, with

$$\mathcal{H}_{ab}(A, B, C) = -\frac{1}{2} \left[\frac{(m_{jj}^2 - m_{\eta_a}^2)(m_{ll}^2 - m_{\eta_a}^2)}{(m_{\eta_a}^2 - m_{\eta_b}^2)(m_{\eta_a}^2 - m_X^2)} A - \frac{(m_{jj}^2 - m_{\eta_b}^2)(m_{ll}^2 - m_{\eta_b}^2)}{(m_{\eta_a}^2 - m_{\eta_b}^2)(m_{\eta_b}^2 - m_X^2)} B \right]$$

$$+ \frac{(m_X^2 - m_{jj}^2)(m_X^2 - m_{ll}^2)}{(m_X^2 - m_{\eta_a}^2)(m_X^2 - m_{\eta_b}^2)} C \Big] \quad , \quad (20)$$

where the mass, m_X , is given by $m_X^2 = \frac{1}{2}(m_{jj}^2 + m_{ll}^2)$. The expression in eq. (19) collapses down to the isospin-symmetric QCD expression given in eq. (15) in the limit, $m_j, m_l, m_u, m_d \rightarrow \overline{m}$. Wavefunction renormalization can be performed for those particles on their mass-shell using (expressions for w_p and w_n are given in Ref. [20] and w_π in the isospin limit is given in Ref. [17]),

$$\begin{aligned} w_\pi &= \frac{1}{3} [-L_{ju} - L_{jd} - L_{lu} - L_{ld} + 2R_{\eta_u, \eta_d} - R_{\eta_u, \eta_u} - R_{\eta_d, \eta_d}] \\ w_p &= g_A^2 (L_{ud} + L_{uu} + 2L_{ju} + 2L_{lu} + 3R_{\eta_u, \eta_u}) \\ &\quad + g_1 g_A (2L_{uu} - L_{ud} + L_{ju} + L_{lu} + 3R_{\eta_u, \eta_u} + 3R_{\eta_u, \eta_d}) \\ &\quad + \frac{g_1^2}{4} (L_{uu} - 5L_{ud} + 2L_{lu} + 3L_{ld} + 2L_{ju} + 3L_{jd} + 3R_{\eta_u, \eta_u} + 6R_{\eta_u, \eta_d} + 3R_{\eta_d, \eta_d}) \\ &\quad + \frac{1}{3} g_{\Delta N}^2 (5J_{ud} + J_{uu} + J_{ju} + J_{lu} + 2J_{jd} + 2J_{ld} + 2\mathcal{T}_{\eta_u, \eta_u} + 2\mathcal{T}_{\eta_d, \eta_d} - 4\mathcal{T}_{\eta_u, \eta_d}) \\ w_n &= g_A^2 (L_{dd} + L_{ud} + 2L_{jd} + 2L_{ld} + 3R_{\eta_d, \eta_d}) \\ &\quad + g_1 g_A (2L_{dd} - L_{ud} + L_{jd} + L_{ld} + 3R_{\eta_u, \eta_d} + 3R_{\eta_d, \eta_d}) \\ &\quad + \frac{g_1^2}{4} (L_{dd} - 5L_{ud} + 2L_{jd} + 3L_{ju} + 2L_{ld} + 3L_{lu} + 3R_{\eta_u, \eta_u} + 6R_{\eta_u, \eta_d} + 3R_{\eta_d, \eta_d}) \\ &\quad + \frac{1}{3} g_{\Delta N}^2 (5J_{ud} + J_{dd} + 2J_{ju} + 2J_{lu} + J_{jd} + J_{ld} + 2\mathcal{T}_{\eta_u, \eta_u} + 2\mathcal{T}_{\eta_d, \eta_d} - 4\mathcal{T}_{\eta_u, \eta_d}) \quad , \quad (21) \end{aligned}$$

by adding a contribution

$$\delta^{(PQ)} \Gamma_j = -\frac{1}{16\pi^2 f^2} \rho w_j \quad . \quad (22)$$

V. $h_{\pi NN}^{(1)}$ AT ONE LOOP WITH LATTICE KINEMATICS

The analysis of the previous section will not be as useful in determining $h_{\pi NN}^{(1)}$ from the lattice as one would naively assume³. While the $P_\pi^\mu = 0$ limit is natural to use from the viewpoint of a momentum and m_q expansion, the fact that lattice simulations only measure on-shell to on-shell amplitudes means that the pions and nucleons are on their mass-shells in both the initial and final states. The extraction of $h_{\pi NN}^{(1)}$ from $N \rightarrow N\pi$ requires an injection of energy at the PV weak vertex which can occur because the weak operator is inserted on one time-slice only. Therefore, we must include contributions from operators that are total derivatives, which usually vanish. Recently, chiral perturbation theory has been used to describe $K \rightarrow \pi\pi$ with the kinematics appropriate for a lattice determination of the matrix elements of the relevant four-quark operators, $m_K^{\text{latt}} = m_\pi^{\text{latt}}$ and $m_K^{\text{latt}} = 2m_\pi^{\text{latt}}$, including

³We are indebted to Steve Sharpe for making this point clear to us.

the necessary total derivative terms [30]. In QCD, the LO Lagrange density describing PV interactions is given in eq. (6), while the Lagrange density at NLO is

$$\mathcal{L}_{\text{wk}}^{(NLO)} = h_D^{(1)} \frac{1}{4} i v \cdot D \bar{N} [X_L^3 - X_R^3] N \quad , \quad (23)$$

where v^μ is the nucleon four-velocity. This is the leading contribution from a heavy baryon reduction of $iD^\mu \bar{N} \gamma_\mu [X_L^3 - X_R^3] N$. Given baryon number conservation, the total derivative gives a non-zero contribution from the energy and momentum injected by the $X_L^3 - X_R^3$ insertion. Working in the frame where the initial state nucleon (proton) is at rest, $v^\mu = (1, 0, 0, 0)$, the amplitude at NLO resulting from eq. (6) and eq. (23) is

$$\mathcal{A}_{\bar{n}p\pi} = \langle n\pi | i \int d^3\mathbf{x} \mathcal{L}^{\Delta I=1}(E) | p \rangle = -\bar{U}_n \left[h_{\pi NN}^{(1)} + h_D^{(1)} \frac{E}{f} \right] U_p \quad . \quad (24)$$

where E is the energy injected by the weak vertex. In order to produce an on-shell $n\pi$ final state, the injected energy must exceed $E \geq m_\pi + M_n - M_p$. Near threshold, where the final state neutron and pion are at rest and $E = m_\pi + M_n - M_p$, the contribution from the total-derivative operator, $h_D^{(1)}$, scales as $\sim m_q^{1/2}$, and is formally dominant over the loop corrections and counterterms of the previous section.

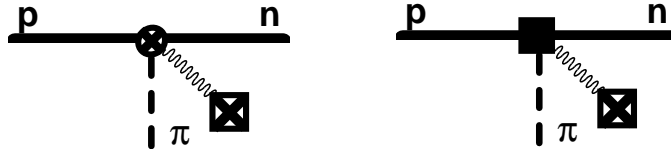


FIG. 2. Tree-level contributions to the parity-violating vertex with lattice kinematics. The crossed circle denotes an insertion of the parity-violating pion-nucleon operators with coefficients $W_{1,2}$ in eq. (10). The solid square denotes an insertion of the energy-momentum dependent operators with coefficients $W_{D1,D2}$ in eq. (25). The crossed-box denotes an insertion of energy-momentum at the weak vertex.

In PQQCD, the lagrange density describing PV interactions at NLO is

$$\begin{aligned} \mathcal{L}_{\text{wk}}^{(NLO)} = & -i \frac{W_{D1}}{4} v \cdot D \left(\bar{\mathcal{B}} \mathcal{B} \left[{}^{(PQ)} X_L^3 - {}^{(PQ)} X_R^3 \right] \right) \\ & - i \frac{W_{D2}}{4} v \cdot D \left(\bar{\mathcal{B}} \left[{}^{(PQ)} X_L^3 - {}^{(PQ)} X_R^3 \right] \mathcal{B} \right) . \end{aligned} \quad (25)$$

The one-loop calculation of the previous section, with minor modifications, provides the leading non-analytic contributions arising at N²LO in the chiral expansion. All other contributions are formally suppressed in the chiral limit. The matrix element at one-loop can be written as, keeping only leading non-analytic terms,

$${}^{(PQ)} \mathcal{A}_{\bar{n}p\pi^+} = \bar{U}_n \left[\bar{\rho} + \frac{1}{16\pi^2 f^2} \left(\bar{\eta}^0 - \frac{1}{2} \bar{\rho} [w_p + w_n + w_\pi] + h_j \bar{\eta}^j + h_l \bar{\eta}^l \right) \right] U_p \quad , \quad (26)$$

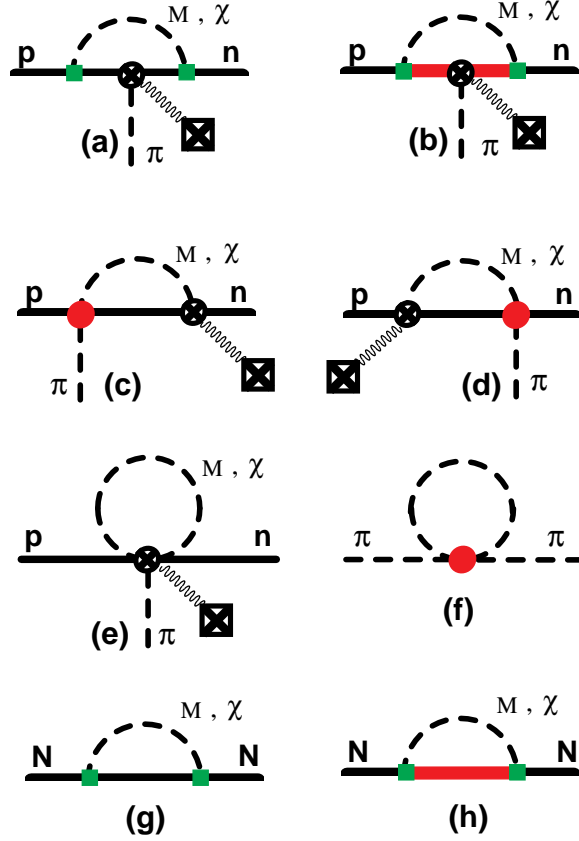


FIG. 3. One-loop graphs that give contributions of the form $\sim m_Q \log m_Q$ to the momentum independent parity-violating interaction $h_{\pi NN}^{(1)}$. A solid, thick-solid and dashed line denote a **70**-nucleon, **44**-resonance, and a meson, respectively. The small solid squares denote an axial coupling given in eq.(12), while the crossed circle denotes an insertion of the parity-violating pion-nucleon operators with coefficients $W_{1,2,3}$ in eq. (10). The solid circle denotes an insertion of the strong two-pion vertex from the nucleon kinetic energy term. The crossed-box denotes an insertion of energy-momentum at the weak vertex. Diagrams (a) to (e) contribute to vertex renormalization while diagrams (f) to (h) contribute to wavefunction renormalization.

where the wavefunction renormalization contributions, w_i , can be found in eq. (21). The diagrams in Fig. 3 give, retaining only the leading non-analytic contributions and working in the frame where the initial state proton is at rest,

$$\begin{aligned}
\bar{\rho} &= \rho - \frac{E}{3f} (2W_{D1} - W_{D2}) \\
\bar{\eta}^0 &= \eta^0 + \frac{\rho}{4} [\tilde{L}_{ud}^{(-)} - \tilde{L}_{dd}^{(-)} + \tilde{L}_{jd}^{(-)} + \tilde{L}_{ld}^{(-)} + \tilde{L}_{ud}^{(+)} - \tilde{L}_{uu}^{(+)} + \tilde{L}_{ju}^{(+)} + \tilde{L}_{lu}^{(+)}] \\
\bar{\eta}^j &= \eta^j + \frac{\rho}{4} [\tilde{L}_{uu}^{(+)} - \tilde{L}_{ju}^{(+)} - \tilde{L}_{ud}^{(-)} + \tilde{L}_{jd}^{(-)}] \\
\bar{\eta}^l &= \eta^l + \frac{\rho}{4} [\tilde{L}_{ud}^{(+)} - \tilde{L}_{lu}^{(+)} - \tilde{L}_{dd}^{(-)} + \tilde{L}_{ld}^{(-)}] \quad , \quad (27)
\end{aligned}$$

where ρ , η^0 , η^j and η^l are given in eq. (19). The functions $\tilde{L}_{ij}^{(\pm)} = \tilde{L}(m_{ij}, \pm E, \mu)$ are

$$\tilde{L}(m, +E, \mu) = -4E \left[E \log \left(\frac{m^2}{\mu^2} \right) - \sqrt{E^2 - m^2} \log \left(\frac{-E - \sqrt{E^2 - m^2 + i\epsilon}}{-E + \sqrt{E^2 - m^2 + i\epsilon}} \right) \right] . \quad (28)$$

Note that these functions are enhanced by a chiral logarithm compared with contributions from local counterterms in the chiral limit. When $E = \pm m_\pi$, corresponding to the production of a nucleon and pion at rest, $\tilde{L}(m, \pm m, \mu) = -4m^2 \log(m^2/\mu^2)$. The additional non-analytic contributions in eq. (27) result from modifications to diagrams (c) and (d) in Fig. 3, with the other diagrams unchanged.

In the limit where $m_{j,l,u,d} \rightarrow \bar{m}$, this matrix element reduces down to that of QCD,

$$\begin{aligned} \mathcal{A}_{\bar{n}p\pi^+} &= \bar{U}_n \left[-h_{\pi NN}^{(1)} - h_D^{(1)} \frac{E}{f} \right. \\ &\left. + \frac{1}{16\pi^2 f^2} \left((6g_A^2 + 4g_{\Delta N}^2) h_{\pi NN}^{(1)} L_\pi + \frac{20}{9} g_{\Delta N}^2 h_{\pi\Delta\Delta}^{(1)} J_\pi - \frac{1}{2} (\tilde{L}_\pi^{(+)} + \tilde{L}_\pi^{(-)}) h_{\pi NN}^{(1)} \right) \right] U_p . \quad (29) \end{aligned}$$

We have not given the numerous counterterms that are expected to appear at N²LO whose μ -dependence will exactly cancel that of the one-loop expressions in eq. (26). The counterterms are expected to make contributions that are smaller than those of the one-loop graphs when a renormalization scale of $\mu \sim \Lambda_\chi$ is chosen, where Λ_χ is the chiral symmetry breaking scale.

For an energy injection of $E > m_\pi + M_n - M_p$, the amplitude develops an imaginary part due to the rescattering of the pion in the intermediate state (final-state interactions). Therefore, in accordance with the Maiani-Testa theorem [31], the simulations must be done at threshold, with $E = m_\pi + M_n - M_p$.

VI. THE ANAPOLE MOMENT AND FORM FACTOR OF THE NUCLEON

An object that plays an important role in PV eH scattering is the anapole moment of H , where H denotes a generic hadron. The dominant PV contributions to eH scattering arise not only from tree-level Z^0 -exchange between H and the electron, but also from the exchange of a photon along with hadronic PV from the four-quark operators in eq. (2). For the proton, there is a contribution to the matrix element of the electromagnetic current in the presence of hadronic PV interactions, of the form

$$\langle p | j_{\text{em}}^\mu(q) | p \rangle = \frac{2}{M_p^2} A_p(q^2) \bar{U}_p \left(S^\mu q^2 - S \cdot q q^\mu \right) U_p , \quad (30)$$

where $A_p(q^2)$ denotes the anapole form factor (the anapole moment is defined to be $A_p(0)$) of the proton. While such electromagnetic contributions vanish for on-shell photons, they give rise to local operators involving the proton and e (or whatever charged probe is involved in the process). In QCD, the anapole moment and form factor of the proton have been computed in χ PT [23,32–35], and are dominated by the $h_{\pi NN}^{(1)}$ coupling (assuming that it is not anomalously small compared to estimates based on naive dimensional analysis). Further, the anapole moments of a few nuclei have been studied theoretically (e.g. Ref. [36]). The proton anapole form factor at LO in χ PT is found to be [33,34]

$$\begin{aligned}
A_p(q^2) &= +\frac{eg_A h_{\pi NN}^{(1)} M_N^2}{48\pi f} \tilde{A}_{\pi^+}(q^2) \\
\tilde{A}_{\pi^+}(q^2) &= \tilde{A}(q^2, m_{\pi^+}) = \frac{12}{(\sqrt{-q^2})^3} \left[\left(m_{\pi^+}^2 - \frac{q^2}{4} \right) \tan^{-1} \left(\frac{\sqrt{-q^2}}{2m_{\pi^+}} \right) - \frac{m_{\pi^+} \sqrt{-q^2}}{2} \right] \\
&\rightarrow \frac{1}{m_{\pi^+}} + \frac{q^2}{20m_{\pi^+}^3} + \dots, \tag{31}
\end{aligned}$$

where the $q^2 \rightarrow 0$ limit reproduces the anapole moment calculation of Ref. [32].

While lattice computations of the proton anapole form factor are of somewhat secondary importance compared to the computation of $h_{\pi NN}^{(1)}$, it would be extremely interesting to have a lattice QCD determination. To this end, we present expressions for the anapole moment of the proton in two-flavor PQQCD. The LO contribution to the proton anapole form factor, arising from the one-loop diagrams shown in Fig. 4, is

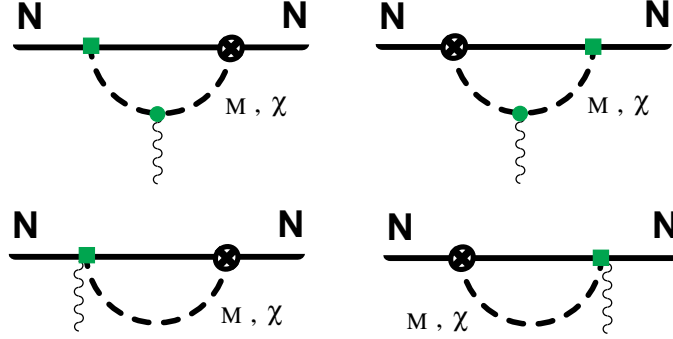


FIG. 4. One-loop graphs that give the leading contribution to the anapole moment and form factor of the nucleon. A solid and dashed line denote a $\mathbf{70}$ -nucleon and a meson, respectively. The solid-squares denote an axial coupling given in eq.(12), while the crossed circle denotes an insertion of the parity-violating pion-nucleon operators with coefficients $W_{1,2}$ in eq. (10).

$$\begin{aligned}
A_p^{(PQ)}(k^2) &= +\frac{eM_N^2}{48\pi f} \left[g_A \left[\frac{1}{3} (2W_1 - W_2) \tilde{A}_{ud} \right. \right. \\
&\quad + W_1 \left[\frac{1}{6} + \frac{1}{4} q_j h_j - \frac{1}{4} q_j - \frac{1}{6} h_j \right] (\tilde{A}_{ju} - \tilde{A}_{uu}) \\
&\quad \left. \left. + W_1 \left[\frac{1}{6} + \frac{1}{4} q_l h_l - \frac{1}{4} q_l - \frac{1}{6} h_l \right] (\tilde{A}_{lu} - \tilde{A}_{ud}) \right] \right] \\
&\quad + g_1 \left[\frac{1}{72} (W_1 (4\tilde{A}_{ju} + \tilde{A}_{ld} + 4\tilde{A}_{lu} - 5\tilde{A}_{ud} - 4\tilde{A}_{uu} - \tilde{A}_{dd} + \tilde{A}_{jd})) \right. \\
&\quad \left. + W_2 (4\tilde{A}_{ju} + 4\tilde{A}_{ld} + 4\tilde{A}_{lu} - 8\tilde{A}_{ud} - 4\tilde{A}_{uu} - 4\tilde{A}_{dd} + 4\tilde{A}_{jd}) \right) \\
&\quad + \frac{h_j}{72} (W_1 (4\tilde{A}_{uu} - \tilde{A}_{ud} - 4\tilde{A}_{ju} + \tilde{A}_{jd})) + 4W_2 (\tilde{A}_{uu} - \tilde{A}_{ud} - \tilde{A}_{ju} + \tilde{A}_{jd})) \\
&\quad + \frac{h_l}{72} (W_1 (4\tilde{A}_{ud} - \tilde{A}_{dd} - 4\tilde{A}_{lu} + \tilde{A}_{ld})) + 4W_2 (\tilde{A}_{ud} - \tilde{A}_{dd} - \tilde{A}_{lu} + \tilde{A}_{ld})) \\
&\quad \left. + \frac{q_j}{24} (W_1 (2\tilde{A}_{uu} - \tilde{A}_{ud} - 2\tilde{A}_{ju} + \tilde{A}_{jd})) + W_2 (2\tilde{A}_{uu} - 4\tilde{A}_{ud} - 2\tilde{A}_{ju} + 4\tilde{A}_{jd})) \right]
\end{aligned}$$

$$\begin{aligned}
& + \frac{q_l}{24} \left(W_1 \left(2\tilde{A}_{ud} - \tilde{A}_{dd} - 2\tilde{A}_{lu} + \tilde{A}_{ld} \right) + W_2 \left(2\tilde{A}_{ud} - 4\tilde{A}_{dd} - 2\tilde{A}_{lu} + 4\tilde{A}_{ld} \right) \right) \\
& + \frac{q_j h_j}{24} \left(W_1 \left(2\tilde{A}_{ju} + \tilde{A}_{jd} - 2\tilde{A}_{uu} - \tilde{A}_{ud} \right) + 2W_2 \left(\tilde{A}_{ju} + 2\tilde{A}_{jd} - \tilde{A}_{uu} - 2\tilde{A}_{ud} \right) \right) \\
& + \frac{q_l h_l}{24} \left(W_1 \left(2\tilde{A}_{lu} + \tilde{A}_{ld} - 2\tilde{A}_{ud} - \tilde{A}_{dd} \right) + 2W_2 \left(\tilde{A}_{lu} + 2\tilde{A}_{ld} - \tilde{A}_{ud} - 2\tilde{A}_{dd} \right) \right) \Big] \\
& \quad] , \tag{32}
\end{aligned}$$

where we have used the short-hand $\tilde{A}_x = \tilde{A}_x(q^2)$ and we have used the electric-charge matrix in PQCD,

$$\mathcal{Q}^{(PQ)} = \text{diag} \left(+\frac{2}{3}, -\frac{1}{3}, q_j, q_l, q_j, q_l \right) , \tag{33}$$

where q_j and q_l are arbitrary charges. The form factor in eq. (32) clearly reduces to the QCD expression in eq. (31) in the appropriate limit.

VII. CONCLUSIONS

With a new generation of experiments designed to determine the PV nucleon-nucleon interaction, it is time for a lattice QCD calculation of the flavor-conserving PV coupling $h_{\pi NN}^{(1)}$. Near future lattice simulations will be partially-quenched with quark masses significantly larger than those of nature. Therefore we have presented the one-loop level expressions required for the extraction of $h_{\pi NN}^{(1)}$, both with vanishing pion four-momentum and with lattice kinematics. Furthermore, we have –with extreme optimism– given the one-loop expressions necessary to determine the proton anapole moment and form factor.

ACKNOWLEDGMENTS

We thank Steve Sharpe for very illuminating discussions and critical comments on this work. This work is supported in part by the U.S. Department of Energy under Grants No. DE-FG03-97ER4014.

REFERENCES

- [1] D.T. Spayde *et al.*, (SAMPLE Collaboration), *Phys. Rev. Lett.* **84**, 1106 (2000); M. L. Pitt [SAMPLE Collaboration], *Nucl. Phys.* **A684**, 333 (2001); R. Hasty *et al.* [SAMPLE Collaboration], *Science* **290**, 2117 (2000).
- [2] S. L. Gilbert, M. C. Noecker, R. N. Watts, C. E. Wieman, *Phys. Rev. Lett.* **55**, 2680 (1985); S. L. Gilbert, C. E. Wieman, *Phys. Rev.* **A34**, 792 (1986); M. C. Noecker, B. P. Masterson, C. E. Wieman, *Phys. Rev. Lett.* **61** (1988); C. S. Wood, UMI-97-25806-mc (microfiche), 1997. (Ph.D.Thesis); C. S. Wood, S. C. Bennet, D. Cho, B. P. Masterson, J. L. Roberts, C. E. Tanner, and C. E. Wieman, *Science* **275**, 1759 (1997); S. C. Bennett and C. E. Wieman *Phys. Rev. Lett.* **82**, 2484 (1999).
- [3] C. A. Barnes, M. M. Lowry, J. M. Davidson, R. E. Marrs, F. B. Moringo, B. Chang, E. G. Adelberger and H. E. Swanson, *Phys. Rev. Lett.* **40**, 840 (1978); P. G. Bizetti, T. F. Fazzini, P. R. Maurenzig, A. Perego, G. Poggi, P. Sona, and N. Taccetti, *Nuovo Cimento* **29**, 167 (1980); G. Ahrens, W. Harfst, J. R. Kass, E. V. Mason, H. Schrober, G. Steffens, H. Waeffler, P. Bock, and K. Grotz, *Nucl. Phys.* **A390**,496 (1982); S. A. Page, H. C. Evans, G. T. Ewan, S. P. Kwan, J. R. Leslie, J. D. Macarthur, W. Mclatchie, P. Skensved, S. S. Wang, H. B. Mak, A. B. Mcdonald, C. A. Barnes, T. K. Alexander, E. T. H. Clifford, *Phys. Rev.* **C35**, 1119 (1987); M. Bini, T. F. Fazzini, G. Poggi, and N. Taccetti, *Phys. Rev. Lett.* **55**, 795 (1985).
- [4] W. C. Haxton and C. E. Wieman, *Ann. Rev. Nucl. Part. Sci.* **51**, 261 (2001).
- [5] P. F. Bedaque and M. J. Savage *Phys. Rev.* **C62**, 018501 (2000); J.-W. Chen, T. D. Cohen and C. W. Kao, *Phys. Rev.* **C64**, 055206 (2001).
- [6] J.-W. Chen and X. D. Ji, *Phys. Rev. Lett.* **86**, 4239 (2001); *Phys. Lett.* **B501**, 209 (2001).
- [7] M. Snow *et al.*, *Nucl. Inst. and Meth.* **440**, 729 (2000).
- [8] C. H. Hyun, T. S. Park and D. P. Min, *Phys. Lett.* **B516**, 321 (2001).
- [9] M. J. Savage, *Nucl. Phys.* **A695**, 365 (2001).
- [10] B. Desplanques, J. F. Donoghue and B. R. Holstein, *Ann. of Phys.* **124**, 449, (1980).
- [11] E. M. Henley, W. Y. Hwang and L. S. Kisslinger, *Phys. Lett.* **B367**, 21 (1996); [Erratum-*ibid.* **B440**, 449 (1996)]; *Phys. Lett.* **B440**, 449 (1998).
- [12] S. R. Sharpe, *Nucl. Phys.* **B17** (Proc. Suppl.), 146 (1990).
- [13] S. R. Sharpe, *Phys. Rev.* **D46**, 3146 (1992).
- [14] C. Bernard and M. F. L. Golterman, *Phys. Rev.* **D46**, 853 (1992).
- [15] J. N. Labrenz and S. R. Sharpe, *Phys. Rev.* **D54**, 4595 (1996).
- [16] M. J. Savage, *Nucl. Phys.* **A700**, 359 (2002).
- [17] S. R. Sharpe and N. Shores, *Phys. Rev.* **D62**, 094503 (2000); *Nucl. Phys. Proc. Suppl.* **83**, 968 (2000); M. F. L. Golterman and K.-C. Leung, *Phys. Rev.* **D57**, 5703 (1998). S. R. Sharpe, *Phys. Rev.* **D56**, 7052 (1997); C. W. Bernard and M. F. L. Golterman, *Phys. Rev.* **D49**, 486 (1994).
- [18] S. R. Sharpe and N. Shores, *Int. J. Mod. Phys.* **A16S1C**, 1219 (2001); *Phys. Rev.* **D64**, 114510 (2001).
- [19] J.-W. Chen and M. J. Savage, [hep-lat/0111050](#).
- [20] S. R. Beane and M. J. Savage, [hep-lat/0203003](#).
- [21] G. Altarelli, R. K. Ellis, L. Maiani and R. Petronzio, *Nucl. Phys.* **B88**, 215 (1975);

- H. Galic, B. Guberina and D. Tadic, *Phys. Rev.* **D14**, 2327 (1976); J. F. Donoghue, *Phys. Rev.* **D13**, 2064 (1976); R. Miller and B. McKellar, *Phys. Rep.* **106**, 169 (1984).
- [22] J. Dai, M. J. Savage, J. Liu and R. P. Springer, *Phys. Lett.* **B271**, 403 (1991).
- [23] D. B. Kaplan and M. J. Savage, *Nucl. Phys.* **A556**, 653 (1993).
- [24] B. Desplanques, *Phys. Rept.* **297**, 1 (1998); nucl-th/0006065.
- [25] S.-L. Zhu, S. J. Puglia, B. R. Holstein, and M. J. Ramsey-Musolf *Phys. Rev.* **D63**, 033006 (2001).
- [26] M. F. L. Golterman and E. Pallante, *JHEP* **0110**, 037 (2001); *Nucl. Phys. Proc. Suppl.* **106**, 335 (2002); hep-lat/0108029.
- [27] E. Jenkins and A. V. Manohar, *Phys. Lett.* **B255**, 558 (1991).
- [28] E. Jenkins and A. V. Manohar, *Phys. Lett.* **B259**, 353 (1991).
- [29] E. Jenkins, *Nucl. Phys.* **B368**, 190 (1992).
- [30] Ph. Boucaud *et al*, *Nucl. Phys. Proc. Suppl.* **106**, 329 (2002); J. Laiho and A. Soni, hep-ph/0203106.
- [31] L. Maiani and M. Testa, *Phys. Lett.* **B245**, 585 (1990).
- [32] W. C. Haxton, E. M. Henley and M. J. Musolf, *Phys. Rev. Lett* **63**, 949 (1989).
- [33] M. J. Savage and R. P. Springer, *Nucl. Phys.* **A644**, 235 (1998); **A657**, 457 (1999)(E); *Nucl. Phys.* **A686**, 413 (2001);
- [34] C. M. Maekawa and U. van Kolck, *Phys. Lett.* **B478**, 73 (2000).
- [35] C. M. Maekawa, J. S. Veiga and U. van Kolck, *Phys. Lett.* **B488**, 167 (2000); S.-L. Zhu, S. J. Puglia, B. R. Holstein, M. J. Ramsey-Musolf *Phys. Rev.* **D62**, 033008 (2000).
- [36] W. C. Haxton, C. P. Liu and M. J. Ramsey-Musolf, nucl-th/0109014; *Phys. Rev. Lett.* **86**, 5247 (2001).